

## Glycerol Electrooxidation in Alkaline Medium Using Pd/C, Au/C and PdAu/C Electrocatalysts Prepared by Electron Beam Irradiation

Adriana N. Geraldes,<sup>a</sup> Dionisio F. Silva,<sup>b</sup> Júlio C. M. Silva,<sup>b</sup> Rodrigo F. B. Souza,<sup>b</sup>  
Estevam V. Spinacé,<sup>b</sup> Almir O. Neto,<sup>b</sup> Marcelo Linardi<sup>b</sup> and Mauro C. Santos<sup>\*a</sup>

<sup>a</sup>Laboratório de Eletroquímica e Materiais Nanoestruturados (LEMN), Centro de Ciências Naturais e Humanas (CCNH), Universidade Federal do ABC (UFABC),  
Rua Santa Adélia, 166, 09210-170 Santo André-SP, Brazil

<sup>b</sup>Centro de Célula a Combustível e Hidrogênio (CCCH), Instituto de Pesquisas Energéticas e Nucleares (IPEN), Av. Prof. Lineu Prestes, 2242, 05508-900 São Paulo-SP, Brazil

Eletrrocatalisadores Pd/C, Au/C e PdAu/C com diferentes razões atômicas foram preparados utilizando-se irradiação por feixe de elétrons e testados na oxidação eletroquímica de glicerol em uma célula alcalina a glicerol direto (ADGFC). Os difratogramas de raios X (XRD) evidenciaram a presença de fases ricas em Pd (fcc) e Au (fcc). As análises de voltametria cíclica (CV) e cronoamperometria indicaram que o eletrrocatalisador com razão atômica 50:50 demonstrou atividade superior para a oxidação eletroquímica do glicerol a temperatura ambiente. As análises de infravermelho com transformada de Fourier no modo de refletância total atenuada (ATR-FTIR) *in situ* identificaram como principais produtos da oxidação eletroquímica do glicerol: 1,3-diidroxi-2-propanona, gliceraldeído e glicolato. Os experimentos em célula unitária foram realizados entre 50 e 90 °C e foi constatado que o melhor desempenho aconteceu a 80 °C.

Pd/C, Au/C and PdAu/C electrocatalysts with different atomic ratios prepared using electron beam irradiation were tested for glycerol electrooxidation in single alkaline direct glycerol fuel cell (ADGFC). X-ray diffractograms (XRD) of PdAu/C electrocatalysts showed the presence of Pd (fcc) and Au (fcc) phases. Cyclic voltammetry (CV) and chronoamperometry showed that PdAu/C electrocatalyst with Pd: Au atomic ratio of 50:50 demonstrated superior activity for glycerol electrooxidation, at room temperature. *In situ* Fourier transform infrared spectroscopy by attenuated total reflectance (ATR-FTIR) experiments were performed for the electrocatalysts, identifying oxalate, glycerate ion, 1,3-dihydroxy-2-propanone, glyceraldehyde and glycolate as products of glycerol electrooxidation. Experiments with single ADGFC were carried out from 50 to 90 °C, using Pd/C electrocatalyst; the best performance was obtained at 80 °C.

**Keywords:** alkaline fuel cell, glycerol, Pd/C, PdAu/C, electrocatalysts

### Introduction

Fuel cells have currently attracted enormous attention because they have great potential for mobile, stationary and portable applications.<sup>1</sup> The interest is greater in fuel cells employing alcohols directly (direct alcohol fuel cell, DAFC), because the use of liquid fuels simplifies the fuel delivery system compared to hydrogen-fed fuel cells.<sup>2-6</sup> Methanol has been considered the most promising alcohol and carbon-supported PtRu nanoparticles (PtRu/C electrocatalyst) was shown to be the best electrocatalyst.<sup>7</sup>

The use of glycerol, a non-valued residue of biodiesel production, as fuel may be an interesting alternative, because it is less toxic than methanol and displays relatively lower theoretical energy density, 5.0 kWh kg<sup>-1</sup>, vs. 6.1 kWh kg<sup>-1</sup> for methanol.<sup>8</sup> Alkaline medium should be preferred to acid medium since the electrochemical reaction kinetics occurring at fuel cell electrodes – fuel oxidation<sup>9</sup> and oxygen reduction<sup>9,10</sup> – are favored and lower platinum loadings or platinum-free electrocatalysts could be used.<sup>11</sup> The problem of catalysis is decisive when considering platinum-free anodic catalysts for the partial oxidation of alcohol in alkaline medium. It has been shown that palladium is an active metal for glycerol and/or ethanol

\*e-mail: mauro.santos@ufabc.edu.br

electrooxidation.<sup>8,12-15</sup> On the other hand, gold is generally considered as a poor electrocatalyst in acid medium; however, its activity in alkaline medium is slightly higher. The reactivity of glycerol and ethanol on gold, in alkaline medium, is related to the fact that practically no poisoning species (CO-like species) may be formed and adsorbed on the surface.<sup>16</sup>

The nature, structure and composition of multi-metallic catalysts have, then, an important effect on the alcohol electrooxidation, in terms of activity (energy generation) and selectivity. Considering that the chemical and physical characteristics of these electrocatalysts depend on the preparation procedure, this becomes a key factor regarding their electrochemical activity.<sup>6</sup> The carbon-supported metal nanoparticles have been prepared for fuel cell applications by radiation-induced reduction of precursors of metal ions.<sup>17</sup> Silva *et al.* prepared PtRu/C electrocatalysts for methanol electrooxidation, in acid medium, using gamma irradiation and electron beam irradiation;<sup>18-20</sup> Silva *et al.*<sup>17</sup> also prepared PtSnO<sub>2</sub>/C electrocatalysts for ethanol electrooxidation, in acid medium, using electron beam irradiation. Moreover, Silva *et al.*<sup>20</sup> studied the activity of the electrocatalysts for alcohol oxidation in alkaline medium and showed that PtAu/C electrocatalysts had a better performance for methanol electrooxidation, compared to other electrocatalysts prepared, while PtAuBi/C (50:40:10) demonstrated a superior performance for ethanol electrooxidation in alkaline medium.<sup>20</sup> In recent work, Geraldes *et al.*<sup>21</sup> prepared carbon-supported Pd, Au and bimetallic PdAu (Pd:Au 90:10, 50:50 and 30:70 atomic ratios) using electron beam irradiation. Chronoamperometry (CA) experiments, at room temperature, revealed that PdAu/C electrocatalysts with Pd:Au ratios of 90:10 and 50:50 presented superior activity toward ethanol electrooxidation. *In situ* Fourier transform infrared spectroscopy by attenuated total reflectance (ATR-FTIR) spectroscopy measurements have shown that the mechanism for ethanol electrooxidation is dependent on catalyst composition, leading to different reaction products, such as acetaldehyde and acetate, depending on the number of electrons transferred. Experiments on a single alkaline direct ethanol fuel cell (ADEFC) were conducted between 50 and 90 °C, and the best performance of 44 mW cm<sup>-2</sup> in 2.0 mol L<sup>-1</sup> ethanol was obtained at 85 °C for the Pd:Au 90:10 catalysts.

In this work Pd/C and PdAu/C electrocatalysts with different Pd:Au atomic ratios were tested for glycerol electrooxidation in alkaline medium, using electrochemical techniques at room temperature, and in alkaline direct glycerol fuel cell (ADGFC), from 50 °C to 90 °C. The products and intermediates formed as result of the glycerol

electrooxidation were determined using *in situ* ATR-FTIR measurements.

## Experimental

### Preparation of Pd/C and PdAu/C electrocatalysts

Pd/C and PdAu/C electrocatalysts (20 wt.% of metal loading) were prepared with different Pd:Au atomic ratios using Pd(NO<sub>3</sub>)<sub>2</sub>·2H<sub>2</sub>O (Fluka) and HAuCl<sub>4</sub>·3H<sub>2</sub>O (Fluka) as metal sources, which were dissolved in water/2-propanol solution 50/50 (v/v). After this, Carbon Vulcan® XC72R, used as support, was dispersed in the solution using an ultrasonic bath. The resulting mixtures were submitted (at room temperature and open atmosphere) under stirring to electron beam irradiation (Electron Accelerator's Dynamitron Job 188, IPEN/CNEN-SP) and the total dose applied was 288 kGy (dose rate 1.6 kGy s<sup>-1</sup>, time 3 min). After electron beam irradiation, the mixtures were filtered and the solids (Pd/C and PdAu/C electrocatalysts) were washed with water and dried at 70 °C for 2 h.<sup>18,19,22</sup>

### Material characterization

The Pd:Au atomic ratios were obtained by energy-dispersive X-ray spectroscopy (EDX) using a Philips XL30 scanning electron microscope with a 20 keV electron beam and equipped with EDAX DX-4 microanalyzer. X-ray diffractometry (XRD) analyses were carried out in a Rigaku Miniflex II diffractometer using CuKα (λ = 1.54056 Å). The diffractograms were recorded at 2θ in the range 20-90° with step size of 0.05° and scan time of 2 s per step. The average crystallite size was calculated using the Scherrer equation.<sup>23</sup> Transmission electron microscopy (TEM) was carried out using a JEOL JEM-2100 electron microscope operated at 200 kV. The particle distribution histogram was determined by measuring 150 particles from micrograph.

### Electrocatalyst activity characterization

Electrochemical studies of the electrocatalysts were carried out using the thin porous coating technique.<sup>24</sup> An amount of 20 mg of the electrocatalyst was added to a solution of 50 mL of water containing 3 drops of a 6% polytetrafluoroethylene (PTFE) suspension. The resulting mixture was treated in an ultrasound bath for 10 min, filtered and transferred to the cavity (0.30 mm deep and 0.36 cm<sup>2</sup> area) of the working electrode. The reference electrode was Ag/AgCl and the counter electrode was a platinumized Pt plate. Electrochemical measurements were made using a Microquimica MQPG01 potentiostat/

galvanostat. Cyclic voltammetry (CV) was performed using 1.0 mol L<sup>-1</sup> glycerol in 1.0 mol L<sup>-1</sup> KOH solution saturated with N<sub>2</sub>. Chronoamperometry experiments were performed using 1.0 mol L<sup>-1</sup> glycerol in 1.0 mol L<sup>-1</sup> KOH solution at -0.30 V at room temperature. The currents in cyclic voltammograms and chronoamperograms were normalized *per gram* of metal. The *in situ* ATR-FTIR measurements were carried out using a Varian® 660 IR spectrometer equipped with a mercury cadmium telluride (MCT) detector cooled with liquid N<sub>2</sub>, a PIKE MIRacle diamond/ZnSe crystal plate ATR accessory and a special cell as presented in the literature.<sup>25</sup> The same working electrode used in the electrochemical experiments was used in ATR-FTIR measurements. These experiments were performed at 25 °C in a 1.0 mol L<sup>-1</sup> KOH solution containing 1.0 mol L<sup>-1</sup> glycerol. The spectra were collected as the ratio R:R<sub>0</sub>, where R represents a spectrum at a given potential, and R<sub>0</sub> is the spectrum collected at -0.70 V. Positive and negative directional bands represent gains and losses of species at the sampling potential, respectively. The spectra were computed from 96 interferograms averaged from 2500 to 850 cm<sup>-1</sup> with the spectral resolution set to 8 cm<sup>-1</sup>. Initially, a reference spectrum, R<sub>0</sub>, was measured at -0.70 V, and sample spectra were collected after applying successive potential steps from -0.85 to 0.20 V. The membrane electrode assemblies (MEAs) were prepared by hot pressing a Fumasep-FAA-PEEK membrane (Fumasep® FAA reinforced with PEEK (FuMA-Tech), pretreated in 1.0 mol L<sup>-1</sup> KOH for 24 h) placed between either a Pd/C or PdAu/C prepared in this work as anode (1 mg metal cm<sup>-2</sup> catalyst loading) and a 20 wt.% Pd/C (prepared in this work) cathode (1 mg metal cm<sup>-2</sup> catalyst loading) at 80 °C for 2 min under a pressure of 45 kgf cm<sup>-2</sup>. The ink containing 70 wt.% Pd/C or PdAu/C catalyst and 30 wt.% of 5% Nafion solution was painted in carbon cloth. The MEA was placed between two bipolar plates and assembled in a single fuel cell under 6 Nm torque wrench. The experiments were performed using a test bench from Electrocell Group. The bench allows controlling the fuel cell operating parameters (flow rates, humidification and temperature of the reactants and cell temperature) and performing automatic data acquisition of polarization curves and power density curves in real time. The liquid fuel feeding is made using a Masterflex L/S Cole-Parmer peristaltic pump. The direct glycerol fuel cell performances were determined in a single cell with an area of 5 cm<sup>2</sup>. The temperature was set between 50 to 90 °C for the fuel cell and 85 °C for the oxygen humidifier. The fuel was 1.0 and 2.0 mol L<sup>-1</sup> glycerol solutions with 1.0 and 2.0 mol L<sup>-1</sup> KOH delivered at 1.0 mL min<sup>-1</sup> and the oxygen flow was regulated at 500 mL min<sup>-1</sup>. Polarization curves were obtained by using a CDE electronic load.

## Results and Discussion

The PdAu/C electrocatalysts prepared with different Pd:Au atomic ratios using electron beam irradiation are shown in Table 1.

**Table 1.** Pd:Au atomic ratios the PdAu/C electrocatalysts prepared with different Pd:Au atomic ratios using electron beam irradiation

Pd:Au atomic ratio (nominal)	Pd:Au atomic ratio (EDX)
90:10	91:09
50:50	58:42
30:70	28:72

Initially, the solutions of Pd(II) and Au(III) ions used to prepare the PdAu/C electrocatalysts are colored. After irradiation and separation of the obtained electrocatalysts by filtration, the filtrates became colorless suggesting that all of the metal ions were reduced to metallic Pd and Au and supported on the carbon. In addition to experimental observation, the EDX analyses showed that Pd:Au atomic ratios were very similar to the nominal ones, considering that all electrocatalysts were obtained with 20 wt.% of metal loading.

Figure 1 shows the XRD diffractograms of Pd/C, Au/C and PdAu/C electrocatalysts.

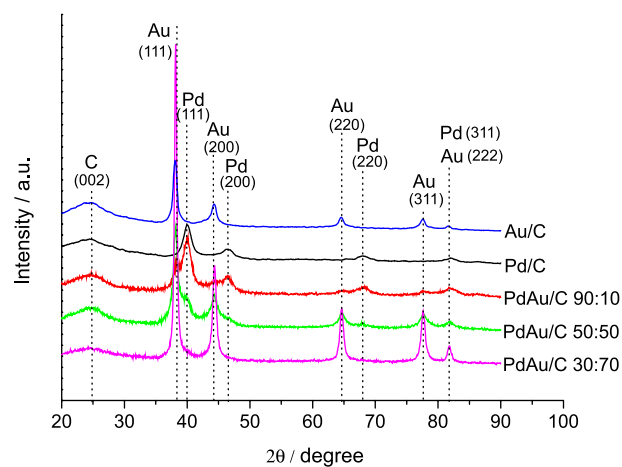


**Figure 1.** X-ray diffractograms of Pd/C, Au/C and PdAu/C (90:10, 50:50 and 30:70 atomic ratios) prepared using electron beam irradiation.

The diffractograms showed a broad peak at about 25°, which was associated with the Vulcan XC72R support. Pd/C electrocatalyst showed four diffraction peaks at about 2θ = 40, 46, 68 and 82° that are associated with the (111), (200), (220) and (311) planes, respectively, which are characteristic of the face-centered cubic (fcc) structure of Pd.<sup>15,16</sup> Au/C electrocatalyst showed five diffraction peaks at about 2θ = 38, 45, 65, 77 and 82° that are associated

with the (111), (200), (220), (311) and (222) planes, respectively, which are characteristic of the fcc structure of Au.<sup>26</sup> PdAu/C (90:10) and (50:50) electrocatalysts showed separated Pd (fcc) and Au (fcc) phases. The PdAu/C (30:70) electrocatalyst showed only the peaks of the Au-rich (fcc) phase, indicating that, for this composition, the Pd atoms could be found as an amorphous phase.<sup>8</sup> The (220) reflections of the Pd (fcc) or Au (fcc) structure were used

to calculate the average crystallite sizes, according to the Scherrer equation.<sup>23</sup> The average crystallite size ranged between 3.0 to 5.2 nm.

Figure 2 shows TEM micrographs and histograms of Pd/C size distribution and PdAu/C (Pd:Au atomic ratios of 90:10, 50:50 and 30:70) electrocatalysts.

TEM micrographs of Pd and Pd:Au atomic ratios of 90:10 and 50:50 electrocatalysts showed a wide distribution

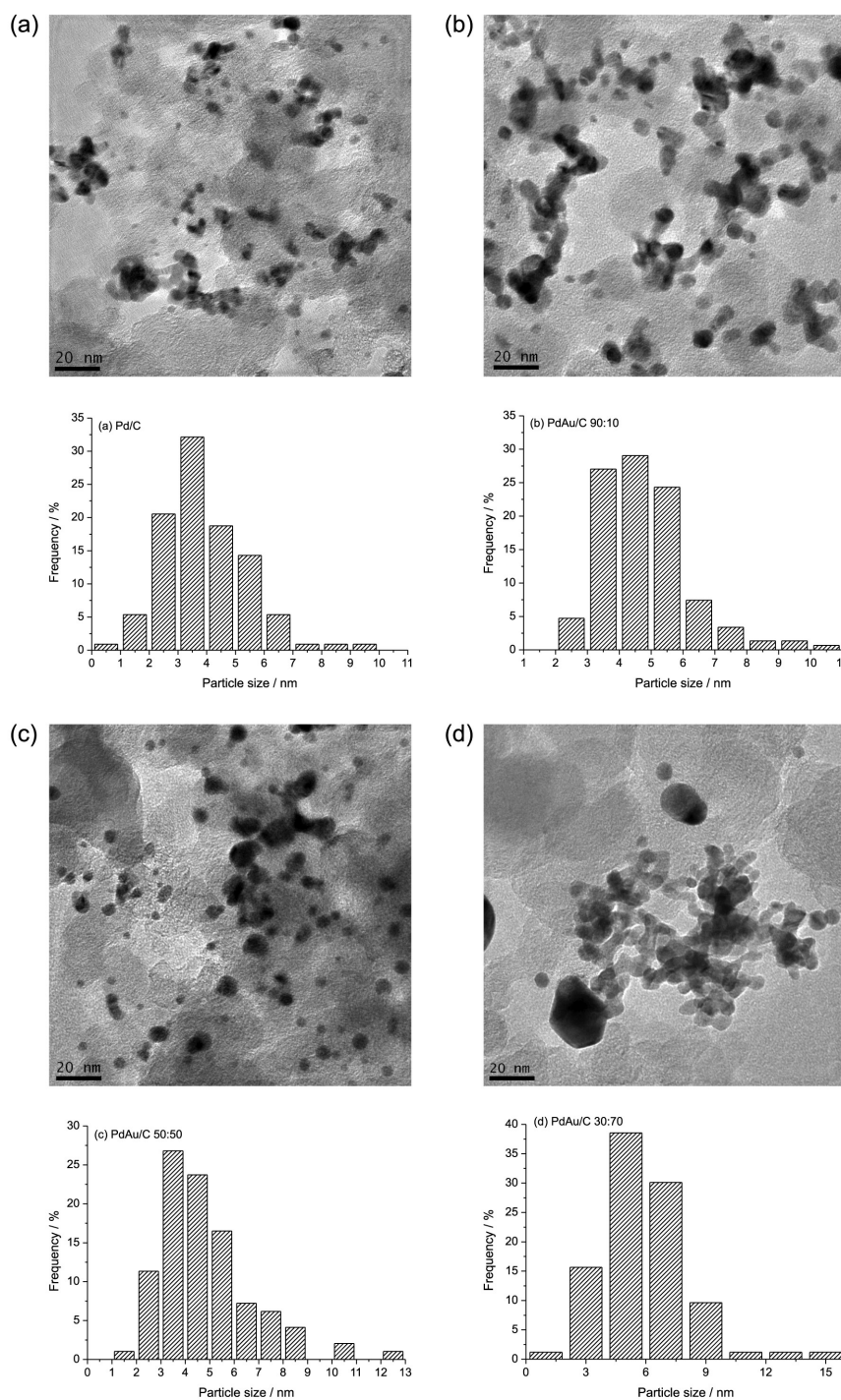


**Figure 2.** TEM micrographs and histograms of (a) Pd/C, (b) PdAu/C (90:10), (c) PdAu/C (50:50), (d) and PdAu/C (30:70) electrocatalysts.

of the nanoparticles on the carbon support with average particle sizes around 4.0 nm and some agglomerates. However, the electrocatalyst PdAu/C 30:70 showed bigger agglomerates and particle sizes around 6.0 nm. Simões *et al.*<sup>8</sup> synthesized monometallic palladium, gold and PdAu/C with atomic ratio of 30:70 and 50:50 nanoparticles supported on carbon. It was shown that the PdAu/C catalysts were alloys and an increase of the crystallite (XRD) and particle (TEM) sizes was observed with the increase of the Au content in the samples.

Figure 3 shows the CV obtained at room temperature in 1.0 mol L<sup>-1</sup> KOH, with a scan rate of 10 mV s<sup>-1</sup> in the presence of 1.0 mol L<sup>-1</sup> glycerol, referring to the Au/C, Pd/C and PdAu/C electrocatalysts, at atomic ratios 90:10, 50:50 and 30:70. The CV responses were normalized *per* gram of metal.

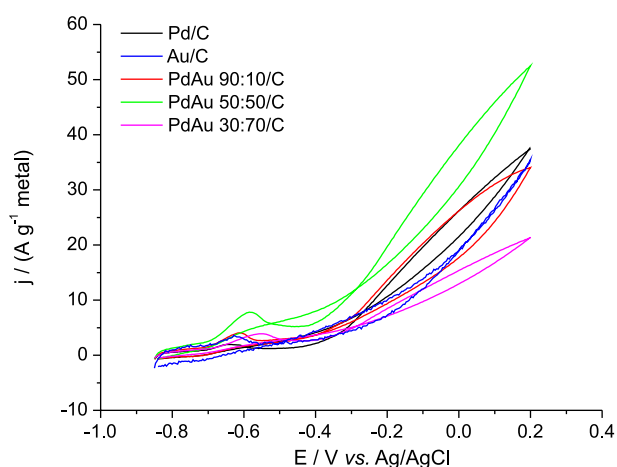
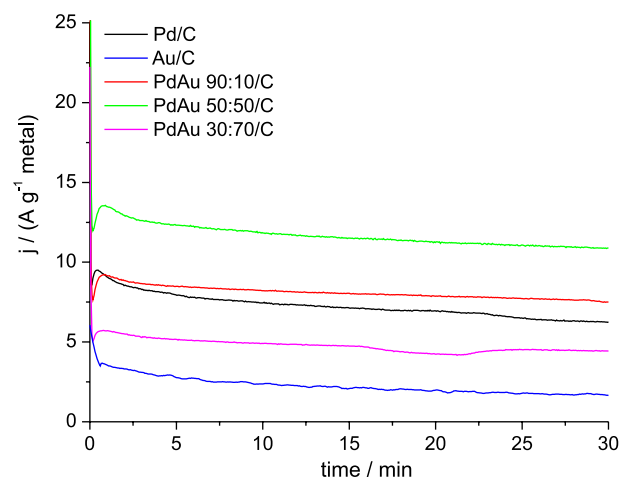


**Figure 3.** Cyclic voltammetry of Pd/C, Au/C and PdAu/C electrocatalysts at atomic ratios 90:10, 50:50 and 30:70 in 1.0 mol L<sup>-1</sup> KOH in 1.0 mol L<sup>-1</sup> glycerol, in a potential range from -0.85 to 0.20 V vs. Ag/AgCl, at a scan rate of 10 mV s<sup>-1</sup>.

The cyclic voltammograms obtained from glycerol electrooxidation on Pd/C and Au/C electrocatalysts show glycerol onset potentials of -0.65 and -0.63 V vs. Ag/AgCl, respectively. The CV of PdAu/C 90:10 electrocatalyst presented lower onset potential (-0.60 V vs. Ag/AgCl), compared to other binary electrocatalysts. PdAu/C 50:50 electrocatalyst showed a higher onset potential (-0.63 V vs. Ag/AgCl) compared to PdAu/C 90:10 electrocatalyst, however, it showed the highest oxidation current and efficiency in the whole potential range evaluated, including the interest region of a fuel cell (-0.45 to -0.30 V vs. Ag/AgCl) directly fed with glycerol. PdAu/C 30:70 electrocatalyst had the lowest current density and higher onset potential. Pd/C, Au/C and PdAu/C (90:10) electrocatalysts showed similar performance in the region of -0.50 and -0.20 V vs. Ag/AgCl. These results show

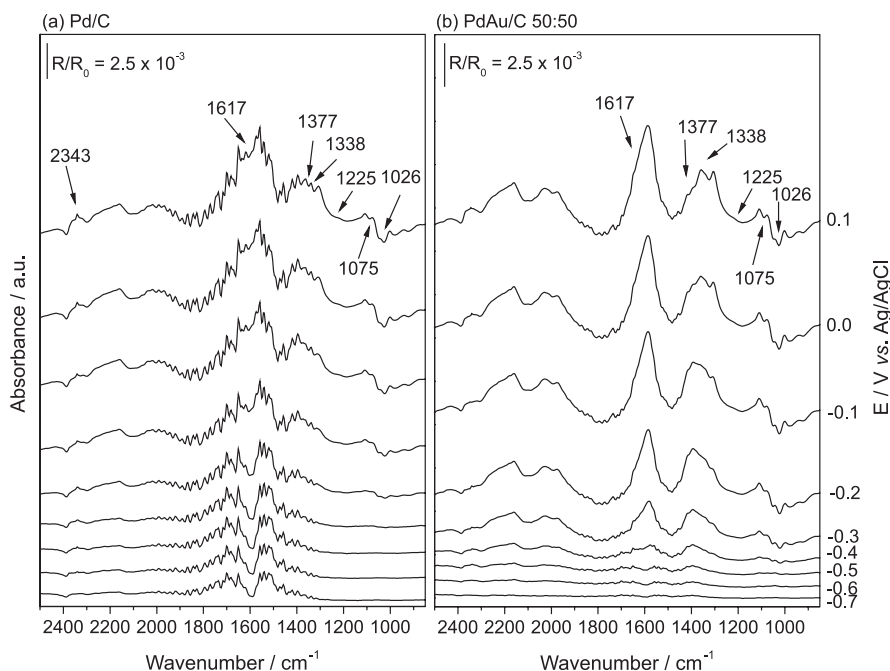
that the addition of Au to Pd/C electrocatalyst promotes a beneficial effect on the performance in the whole potential range. The best performance of the PdAu/C electrocatalysts may be attributed to the bifunctional mechanism where Pd species are available for glycerol adsorption and Au provide oxygen species for the oxidation of the intermediates.<sup>27</sup>

Figure 4 shows the chronoamperometry obtained at room temperature, in solutions of 1.0 mol L<sup>-1</sup> KOH in 1.0 mol L<sup>-1</sup> glycerol, at a fixed potential of -0.30 V vs. Ag/AgCl, for 30 min, concerning the Au/C and PdAu/C electrocatalysts, at atomic ratios 90:10, 50:50 and 30:70.



**Figure 4.** Current-time curves at -0.30 V for Pd/C, Au/C and PdAu/C electrocatalysts, at atomic ratios 90:10, 50:50 and 30:70 in 1.0 mol L<sup>-1</sup> glycerol in 1.0 mol L<sup>-1</sup> KOH.

The chronoamperometry curves are recorded for 30 minutes. The peaks that occur in the first few seconds are due to charging double layer and the instability of the system under the conditions in which the experiment was performed. After this short interval the system stabilizes. For all the electrodes, the measurement shows a slight fall in the current value for the studied electrocatalysts, probably associated with no restoration of fuel and/or degradation or poisoning of the electrode, due to the formation and adsorption of intermediate species generated during the glycerol electrooxidation, in the time interval measured. From the graphs, it may be seen that the Pd/C electrocatalyst presents a more pronounced drop in the density current value, while the PdAu/C electrocatalysts with 90:10, 50:50 and 30:70 atomic ratios are more stable, since the decrease in the current density is less substantial. It may be also observed that the PdAu/C 50:50 electrocatalyst is the most active among all the evaluated ones and PdAu/C 30:70 electrocatalyst provides an oxidation current lower than the pure Pd/C. On the other hand, pure Au/C electrocatalyst exhibits low activity. These results suggest that, in the investigated electrode potential, the addition



**Figure 5.** *In situ* FTIR spectra of (a) Pd/C and (b) PdAu/C 50:50 electrocatalysts, taken in the potential range  $-0.70$  to  $0.20$  V vs. Ag/AgCl, in  $1.0$  mol L $^{-1}$  glycerol in  $1.0$  mol L $^{-1}$  KOH. Each spectrum corresponds to an increase of  $0.10$  V.

of up to 50% of Au at Pd/C electrocatalyst contributes to the activity and stability of Pd-based electrocatalysts, toward glycerol electrooxidation, yielding more efficiency and tolerant to poisoning electrocatalysts. This fact may be attributed to the synergistic effect that gold carries on palladium and to bifunctional mechanism.

To understand the different activities of the prepared electrocatalysts toward glycerol electrooxidation *in situ*, ATR-FTIR analyses were performed for the Pd/C and PdAu/C 50:50 electrocatalysts, aiming to identify the products of glycerol electrooxidation generated during the potential scan between  $-0.70$  to  $0.20$  V vs. Ag/AgCl. The IR spectra were recorded every  $0.10$  V, in  $1.0$  mol L $^{-1}$  glycerol in  $1.0$  mol L $^{-1}$  KOH aqueous solution; these spectra are shown in Figure 5.

In the spectra related to Pd/C, there is some interference due to the surface water or water vapor in the region  $1540$ - $1750$  cm $^{-1}$ .<sup>28</sup> For both spectra, it is observed the appearance of a band at  $1617$  cm $^{-1}$ , related to oxalate.<sup>29</sup> It is also possible to notice the bands at  $1377$  cm $^{-1}$ , attributed to glycerate ion,  $1338$  cm $^{-1}$ , attributed to 1,3-dihydroxy-2-propanone,  $1225$  cm $^{-1}$ , attributed to aldehyde polymers,  $1310$  cm $^{-1}$ , attributed to glyceraldehyde or glycerate ion,  $1026$  cm $^{-1}$ , attributed to glycerol consumption<sup>12</sup> and  $1075$  cm $^{-1}$ , attributed to the production of glycolate.<sup>30</sup> In these spectra, it was also observed the appearance of a discrete band at  $2343$  cm $^{-1}$ , related to CO<sub>2(g)</sub>, subsequently converted to carbonate in the spectrum of Pd/C. To associate the variation of main bands during the electrooxidation

of glycerol, all bands were deconvoluted by Lorentzian line forms, so the intensity and the wavelength of each band could be individually analyzed. The band intensities related to glycerate ion, glyceraldehyde and 1,3 dihydroxyl 2-propanone were plotted in Figure 6.

It is more clearly seen that, in PdAu/C, the glyceraldehyde generation is greater than in Pd/C, in all potential ranges evaluated. Similar results can also be seen in 1,3-dihydroxy-2 propanone (Figure 6c). It was observed that glycerate ion species, using PdAu/C, were produced in  $100$  mV less positive than using Pd/C. However, at  $-0.3$  V (chronoamperometry potential), the glycerate band is higher than PdAu/C: these ions can poison the palladium active sites. Higher kinetics on aldehyde and ketone generation presented by PdAu/C electrocatalyst and higher kinetics on glycerate ion generation on Pd/C may explain the increased performance of PdAu/C electrocatalyst.

The activity of Pd/C electrocatalyst was evaluated using a single fuel cell with geometric area of  $5$  cm $^2$ . The synthesized electrocatalysts were applied as an anodic catalyst for ADGFC, fed with  $1.0$  mol L $^{-1}$  glycerol solution in  $1.0$  mol L $^{-1}$  KOH and a solution of  $2.0$  mol L $^{-1}$  glycerol in  $2.0$  mol L $^{-1}$  KOH, with  $1.0$  mL min $^{-1}$  reactant flow rate and  $1.0$  mg Pd cm $^{-2}$  anodic and cathodic catalytic loading.

Figure 7 shows the single fuel cell performance between  $50$ - $90$  °C, with Pd/C electrocatalyst, fed with  $1.0$  and  $2.0$  mol L $^{-1}$  glycerol in  $1.0$  and  $2.0$  mol L $^{-1}$  KOH solutions.

In order to evaluate the best operation temperature, the fuel cell temperature was set between  $50$  and  $90$  °C,

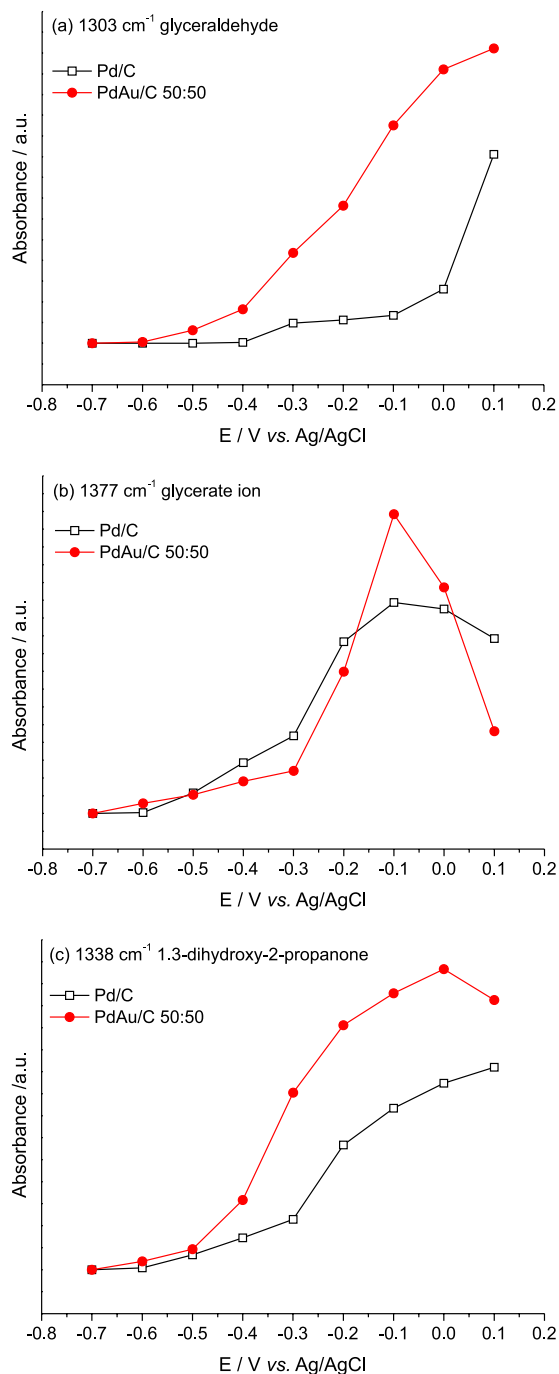


**Figure 6.** Generation of glycerinaldehyde (a), glycerate ion (b) and 1,3-dihydroxy-2-propanone (c) in the Pd/C and PdAu/C 50:50 electrocatalysts, as a function of potential.

85 °C for the oxygen humidifier, and glycerol was fed at room temperature. The performance was significantly improved with the temperature increase. The largest power density was at 80 °C, for both glycerol concentrations. For 1.0 mol L<sup>-1</sup> glycerol in 1.0 mol L<sup>-1</sup> KOH, the open circuit voltage (OCV) of the fuel cell was 0.68 V and power density of 18 mW cm<sup>-2</sup>. The fuel cell fed with 2.0 mol L<sup>-1</sup> glycerol in 2.0 mol L<sup>-1</sup> KOH also presented an increase

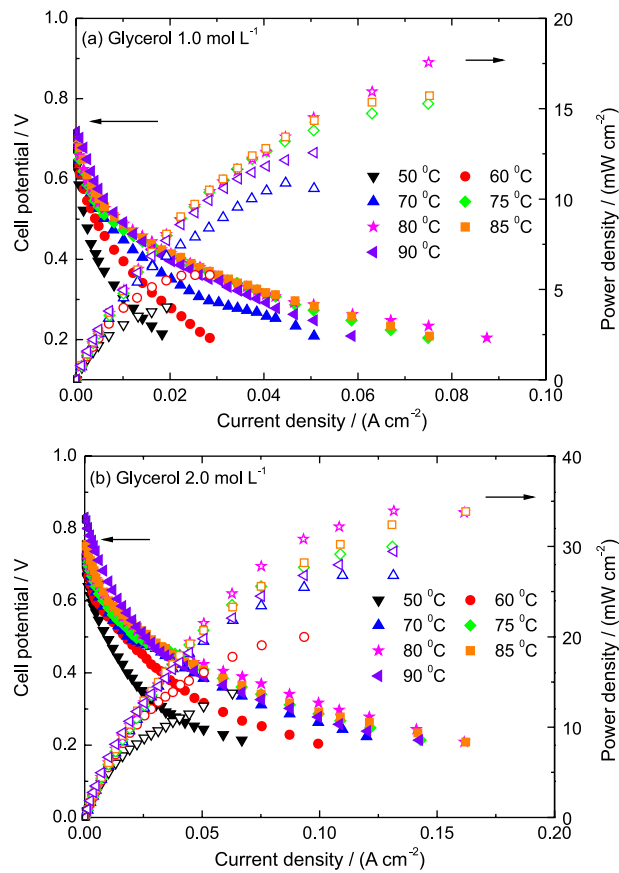


**Figure 7.** Polarization and power density curves of a 5 cm<sup>2</sup> ADGFC at 50 to 90 °C using Pd/C electrocatalyst, fed with (a) 1.0 mol L<sup>-1</sup> glycerol in 1.0 mol L<sup>-1</sup> KOH and (b) 2.0 mol L<sup>-1</sup> glycerol in 2.0 mol L<sup>-1</sup> KOH solutions, anodic and cathodic catalytic loading 1.0 mg metal cm<sup>-2</sup>; Fumasep-FAA3-PEEK membrane and oxygen humidifier temperature at 85 °C.

in cell performance: the OCV and power density values were 0.72 V and 34 mW cm<sup>-2</sup>, respectively. In addition, in both concentrations, when the operation temperature was increased; the decay of current-potential (I-V) curves is less pronounced in the electrochemical kinetics-controlled low current density region (i.e., 0.01 A cm<sup>-2</sup> for 1.0 mol L<sup>-1</sup> glycerol and 0.05 A cm<sup>-2</sup> for 2.0 mol L<sup>-1</sup> glycerol), indicating that the glycerol oxidation kinetics was greatly enhanced at higher temperatures. In the ohmic drop region, associated with the system's electrical resistances, the plot inclination decreases when increasing the temperature, for both glycerol concentrations. It was also observed that both graphs reach maximum current without exponential decay associated with the mass transport limitations: this indicates that the electrode kinetics may be improved without changing physical characteristics, such as porosity and fuel supply, i.e., the losses are associated with the kinetics and the resistivity of the electrodes. After 90 °C, a decrease in cell performance was observed. These results indicate that better reactant diffusion and higher kinetics of the electrode may be achieved at higher temperatures and

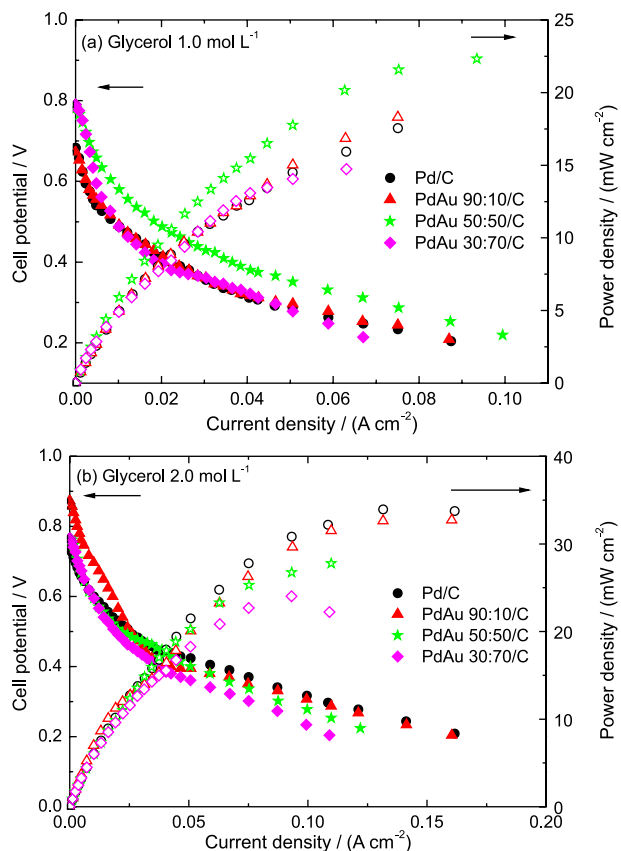


**Figure 8.** Polarizations and power density curves of a 5 cm<sup>2</sup> ADGFC with Pd/C and PdAu/C 90:10, 50:50 and 30:70 atomic ratio electrocatalysts, fed with a solution of (a) 1.0 mol L<sup>-1</sup> glycerol in 1.0 mol L<sup>-1</sup> KOH and (b) 2.0 mol L<sup>-1</sup> glycerol in 2.0 mol L<sup>-1</sup> KOH at 80 °C, using Pd/C and PdAu/C anodic electrocatalysts and Pd/C cathodic electrocatalyst; anodic and cathodic catalyst loading 1 mg metal cm<sup>2</sup>, Fumasep-FAA3-PEEK membrane and oxygen humidifier temperature of 85 °C.

that, above 80 °C, the emergence of new processes, such as dryness, resistivity and diffusion, begin to degrade the performance of the electrodes. The increase of both OCV and power density with increase of the fuel concentration and cell temperature also suggests that the membrane used in MEA has low permeability to glycerol: an increase in the cell operating temperature favors ion mobility in the membrane, increasing the permeability and the occurrence of parallel reactions between the fuel and OH<sup>-</sup> species present in the cathode, creating a potential mix and reducing the cell overall potential. The OCV increase with higher temperature is an indication that the OCV is similar to the reversible potential (which varies with temperature), since there are no losses due to the crossing of species between the two electrodes or internal current.<sup>31</sup> Santasalo-Aarnio *et al.*<sup>32</sup> studied the anion exchange membrane Fumasep® FAA-2. Fuel cell experiments in 1 mol L<sup>-1</sup> methanol with FAA-2 resulted in an OCV of 0.58 V and maximum power density of 0.32 mW cm<sup>-2</sup>; even higher current densities were obtained with greatly concentrated fuels. The authors

concluded that less water is needed for fuel dilution, thereby decreasing the mass of the fuel cell system.

The highest power densities, obtained with the MEA fed with 1.0 mol L<sup>-1</sup> and 2.0 mol L<sup>-1</sup> glycerol, were generated at 80 °C, indicating the best operating temperature of the palladium-based MEAs. Figure 8 shows the performance, at 80 °C, of a single fuel cell with Pd/C and PdAu/C 90:10, 50:50 and 30:70 atomic ratio electrocatalysts, fed with a solution of 1.0 mol L<sup>-1</sup> and 2.0 mol L<sup>-1</sup> glycerol in 1.0 and 2.0 mol L<sup>-1</sup> KOH.

In the 1.0 mol L<sup>-1</sup> glycerol solution (Figure 8a), the polarization and power density measurements show that the OCV of the fuel cell containing Pd/C electrocatalyst was 0.68 V, while the corresponding values for PdAu/C 90:10, 50:50 and 30:70 were 0.67, 0.78 and 0.79 V, respectively. The maximum power density of PdAu 50:50 electrocatalyst (22 mW cm<sup>-2</sup>) is slightly higher than that with Pd/C electrocatalyst (18 mW cm<sup>-2</sup>), while the PdAu 90:10 atomic ratio electrocatalyst showed a power density similar to the Pd/C, overcoming only in the region of high current. It was also noted that the electrocatalyst PdAu/C 30:70 showed a lower power density throughout the potential range examined. The single-cell tests in the 1.0 mol L<sup>-1</sup> solution demonstrate that the addition of up to 50 parts of Au into PdAu/C catalyst may increase its activity for glycerol oxidation reaction in agreement with cyclic voltammetry and chronoamperometry experiments.

In the 2.0 mol L<sup>-1</sup> glycerol solution (Figure 8b), the power density measurements show that the maximum power density of Pd/C and PdAu 90:10 electrocatalysts were similar (34 mW cm<sup>-2</sup>) while PdAu 50:50 and PdAu/C 30:70 electrocatalysts showed lower power density compared to Pd/C throughout the potential range examined. It was also noted that the addition of only up to 10 parts of Au into PdAu/C catalyst might increase its activity for glycerol oxidation reaction. This fact is probably due to the lower amount of palladium active sites for the adsorption of glycerol molecules. Differently from what happened with 1.0 mol L<sup>-1</sup> glycerol, glycerol at higher concentration requires a greater number of palladium active sites because palladium is responsible for adsorption of glycerol molecules and gold is responsible for OH<sup>-</sup> species adsorption, which promote the oxidation of the electrooxidation intermediate glycerol by bifunctional mechanism. Simões *et al.*<sup>8</sup> studied the oxidation of glycerol in PdAu/C electrocatalysts and proposed that the presence of a co-catalyst promotes changes in the mechanism of glycerol electrooxidation and an increase in the activity. Mougnot *et al.*<sup>33</sup> studied PdAu (70:30) catalyst, alternate sputtered PdAuPd (35:30:35) and AuPdAu (15:70:15) materials prepared by plasma deposition of Au and Pd

atoms, on a carbon diffusion layer. The modification of palladium surface by gold atoms leads to an increase in the catalytic activity towards glycerol electrooxidation. The PdAu alloy surface composition has no significant effect on the catalytic activity; however, the presence of non-alloyed gold sites on the material surface leads to the enhancement of the catalytic activity. The mechanism seems to involve glycerol adsorption on palladium surface and hydroxyl species formation on gold surface, leading to catalytic activity enhancement through the bifunctional mechanism. Ilie *et al.*<sup>13</sup> tested the commercial anionic membrane Fumapem® FAA (FuMA-Tech). The tests were performed in a 5 cm<sup>2</sup> cell with identical anode and cathode (Pt (40 wt.%) / C, 2 mg Pt cm<sup>-2</sup> deposited on a diffusion layer carbon cloth with PTFE (15 wt.%) / C). The used fuel composition was 1.0 mol L<sup>-1</sup> glycerol / 4.0 mol L<sup>-1</sup> NaOH, and oxygen was used as oxidant. The power densities achieved with the FuMA-Tech membrane was 13.5 mW cm<sup>-2</sup> at 60 °C, and 7.8 mW cm<sup>-2</sup> at 25 °C.

It is assumed that the reactions involved in an ADGFC working with glycerol-KOH fuel occur with higher kinetics than those in acid fuel cell. Under these circumstances, the possibility of either decreasing the Pt loading or even using non-platinum-based catalysts may be considered. The literature shows that some Pt-based and Pd-based catalysts displayed high catalytic activity for alcohol or polyol electrooxidation in alkaline medium.<sup>13,15,27,34</sup> Moreover, Pd-based bimetallic catalysts seem to be more stable with respect to degradation than pure Pd on carbon black.<sup>13,35,36</sup>

## Conclusions

Pd/C and PdAu/C electrocatalysts with 90:10, 50:50 and 30:70 Pd:Au atomic ratios were prepared. The best operating temperature was evaluated to be around 80 °C, towards glycerol electrooxidation in Pd-based electrocatalysts. The addition of Au is supposed to improve the activity and stability of binary PdAu/C electrocatalysts; however, it is assumed that the best proportion depends on the fuel concentration as well as the cell temperature. The promoting effect of Au has been explained by a bifunctional mechanism, where Au would adsorb and increase the concentration of OH<sup>-</sup> species, on proximity to Pd, favoring the oxidation of glycerol/intermediary adsorbed on the Pd surface. The promoting effect of the second metal on PdAu/C has been explained also by greater formation of glyceraldehyde and glycerate ion species than in Pd/C. The experiments indicated that the glycerol oxidation kinetics was greatly enhanced at higher temperatures. At 80 °C, for 1.0 mol L<sup>-1</sup> glycerol electrooxidation, the best composition was Pd:Au 50:50

and the maximum power density was 22 mW cm<sup>-2</sup> while for 2.0 mol L<sup>-1</sup> glycerol the best composition was Pd:Au 90:10 and the maximum power density was 34 mW cm<sup>-2</sup>.

## Acknowledgments

The authors wish to thank FAPESP (2012/03516-5, 2013/01557-0), CNPq (162669/2013-5, 474913/2012-0, 406612/2013-7), Instituto Nacional de Ciência e Tecnologia (INCT) de Energia e Meio Ambiente (Process Number. 573.783/2008-0) and UFABC for their financial support, CTR and CCTM from IPEN/CNEN-SP for electron beam irradiations and TEM measurements.

## References

1. Barbir, F.; *PEM Fuel Cells*; Academic Press: London, 2013.
2. Shen, S. Y.; Zhao, T. S.; Xu, J. B.; Li, Y. S.; *J. Power Sources* **2010**, *195*, 1001.
3. Neto, A. O.; Dias, R. R.; Tusi, M. M.; Linardi, M.; Spinacé, E. V.; *J. Power Sources* **2007**, *166*, 87.
4. Zhou, W. J.; Li, W. Z.; Song, S. Q.; Zhou, Z. H.; Jiang, L. H.; Sun, G. Q.; Xin, Q.; Poulantitis, K.; Kontou, S.; Tsiakaras, P.; *J. Power Sources* **2004**, *131*, 217.
5. Rousseau, S.; Coutanceau, C.; Lamy, C.; Léger, J.-M.; *J. Power Sources* **2006**, *158*, 18.
6. Antolini, E.; *J. Power Sources* **2007**, *170*, 1.
7. Liu, H.; Song, C.; Zhang, L.; Zhang, J.; Wang, H.; Wilkinson, D. P.; *J. Power Sources* **2006**, *155*, 95.
8. Simões, M.; Baranton, S.; Coutanceau, C.; *Appl. Catal., B* **2010**, *93*, 354.
9. Yang, C. C.; *Int. J. Hydrogen Energy* **2004**, *29*, 135.
10. Wang, Y.; Li, L.; Hu, L.; Zhuang, L.; Lu, J.; Xu, B.; *Electrochim. Commun.* **2003**, *5*, 662.
11. Demarconnay, L.; Coutanceau, C.; Leger, J. M.; *Electrochim. Acta* **2004**, *49*, 4513.
12. Simões, M.; Baranton, S.; Coutanceau, C.; *Appl. Catal., B* **2011**, *110*, 40.
13. Ilie, A.; Simões, M.; Baranton, S.; Coutanceau, C.; Martemianov, S.; *J. Power Sources* **2011**, *196*, 4965.
14. Xu, C.; Zeng, R.; Shen, P. K.; Wei, Z.; *Electrochim. Acta* **2005**, *51*, 1031.
15. Bambagioni, V.; Bianchini, C.; Marchionni, A.; Fillipi, J.; Vizza, F.; Teddy, J.; Serp, P.; Zhiani, M.; *J. Power Sources* **2009**, *190*, 241.
16. Tremiliosi-Filho, G.; Gonzalez, E. R.; Motheo, A. J.; Belgsir, E. M.; Léger, J. M.; Lamy, C.; *J. Electroanal. Chem.* **1998**, *444*, 31.
17. Silva, D. F.; Geraldés, A. N.; Neto, A. O.; Pino, E. S.; Linardi, M.; Spinacé, E. V.; Macedo, W. A. A.; Ardisson, J. D.; *Mater. Sci. Eng., B* **2010**, *175*, 261.

18. Silva, D. F.; Neto, A. O.; Pino, E. S.; Linardi, M.; Spinacé, E. V.; *J. Power Sources* **2007**, *170*, 303.
19. Silva, D. F.; Neto, A. O.; Pino, E. S.; Brandalise, M.; Linardi, M.; Spinacé, E. V.; *Mater. Res.* **2007**, *10*, 367.
20. Silva, D. F.; Geraldés, A. N.; Cardoso, E. Z.; Tusi, M. M.; Linardi, M.; Spinacé, E. V.; Neto, A. O.; *Int. J. Electrochem. Sci.* **2011**, *6*, 3594.
21. Geraldés, A. N.; Silva, D. F.; Pino, E. S.; Silva, J. C. M.; Souza, R. F. B.; Hammer, P.; Spinacé, E. V.; Neto, A. O.; Linardi, M.; Santos, M. C.; *Electrochim. Acta* **2013**, *111*, 455.
22. Spinacé, E. V.; Neto, A. O.; Linardi, M.; Silva, D. F.; Pino, E. S.; Cruz, V. A.; PI 0505416-8, INPI-RJ, 08/12/2005, 2005.
23. Radmilovic, V.; Gasteiger, H. A.; Ross, P. N.; *J. Catal.* **1995**, *154*, 98.
24. Neto, A. O.; Giz, M. J.; Perez, J.; Ticianelli, E. A.; Gonzalez, E. R.; *J. Electrochem. Soc.* **2002**, *149*, A272.
25. Silva, J. C. M.; Parreira, L. S.; Souza, R. F. B.; Calegari, M. L.; Spinacé, E. V.; Neto, A. O.; Santos, M. C.; *Appl. Catal., B* **2011**, *110*, 141.
26. Lee, A. F.; Baddeley, C. J.; Hardacre, C.; Ormerod, R. M.; Lambert, R. M.; *J. Phys. Chem.* **1995**, *99*, 6096.
27. Bianchini, C.; Shen, P. K.; *Chem. Rev.* **2009**, *109*, 4183.
28. Simões, F. C.; dos Anjos, D. M.; Vigier, F.; Léger, J. M.; Hahn, F.; Coutanceau, C.; Gonzalez, E. R.; Tremiliosi-Filho, G.; Andrade, A. R.; Olivi, P.; Kokoh, K. B.; *J. Power Sources* **2007**, *167*, 1.
29. Falase, Z. A.; Garcia, K.; Lau, C.; Atanassov, P.; *Electrochem. Commun.* **2011**, *13*, 1488.
30. Jeffery, D. Z.; Camara, G. A.; *Electrochem. Commun.* **2010**, *12*, 1129.
31. Zeng, Q. H.; Liu, Q. L.; Broadwell, I.; Zhu, A. M.; Xiong, Y.; Tu, X. P.; *J. Membr. Sci.* **2010**, *349*, 237.
32. Santasalo-Aarnio, Z. A.; Hietalab, S.; Rauhalaa, T.; Kallio, T.; *J. Power Sources* **2011**, *196*, 6153.
33. Mougnot, M.; Caillard, A.; Simões, M.; Baranton, S.; Coutanceau, C.; Brault, P.; *Appl. Catal., B* **2011**, *107*, 372.
34. Shen, P. K.; Xu, C.; *Electrochem. Commun.* **2006**, *8*, 184.
35. Tarasevich, M. R.; Bogdanovskaya, V. A.; Kuznetsova, L. N.; Modestov, A. D.; Efremov, B. N.; Chalykh, A. E.; Chirkov, Y. G.; Kapustina, N. A.; Ehrenburg, M. R.; *J. Appl. Electrochem.* **2007**, *37*, 1503.
36. Tarasevich, M. R.; Zhutaeva, G. V.; Bogdanovskaya, V. A.; Radina, M. V.; Ehrenburg, M. R.; Chalykh, A. E.; *Electrochim. Acta* **2007**, *52*, 5108.

Submitted: November 11, 2013

Published online: February 21, 2014

FAPESP has sponsored the publication of this article.